Simple Machine Perfusion Significantly Enhances Hepatocyte Yields of Ischemic and Fresh Rat Livers

Maria-Louisa Izamis,* Candice Calhoun,* Basak E. Uygun,* Maria Angela Guzzardi,*
Gavrielle Price,* Martha Luitje,* Nima Saeidi,* Martin L. Yarmush,*† and Korkut Uygun*

*Center for Engineering in Medicine, Massachusetts General Hospital,
Harvard Medical School, Shriners Hospitals for Children, Boston, MA, USA
†Department of Biomedical Engineering, Rutgers University, Piscataway, NJ, USA

The scarcity of viable hepatocytes is a significant bottleneck in cell transplantation, drug discovery, toxicology, tissue engineering, and bioartificial assist devices, where trillions of high-functioning hepatocytes are needed annually. We took the novel approach of using machine perfusion to maximize cell recovery, specifically from uncontrolled cardiac death donors, the largest source of disqualified donor organs. In a rat model, we developed a simple 3-h room temperature ($20\pm2°C$) machine perfusion protocol to treat nonpremedicated livers exposed to 1 h of warm ($34°C$) ischemia. Treated ischemic livers were compared to fresh, fresh-treated, and untreated ischemic livers using viable hepatocyte yields and in vitro performance as quantitative endpoints. Perfusion treatment resulted in both a 25-fold increase in viable hepatocytes from ischemic livers and a 40% increase from fresh livers. While cell morphology and function in suspension and plate cultures of untreated warm ischemic cells was significantly impaired, treated warm ischemic cells were indistinguishable from fresh hepatocytes. Furthermore, a strong linear correlation between tissue ATP and cell yield enabled accurate evaluation of the extent of perfusion recovery. Maximal recovery of warm ischemic liver ATP content appears to be correlated with optimal flow through the microvasculature. These data demonstrate that the inclusion of a simple perfusion-preconditioning step can significantly increase the efficiency of functional hepatocyte yields and the number of donor livers that can be gainfully utilized.

Key words: Disqualified cardiac death (DCD); Nonheart beating donor (NHBD); Ischemia;
Adenosine triphospate (ATP); Cell isolation

INTRODUCTION

There is a global unmet demand for viable donor livers. For every transplantable organ, there are at least four eligible candidates (32,42). The success of transplantation has led to a 3.6% annual increase in additions to the waiting list, while the availability of transplantable livers has plateaued at 5,000–6,000 per year (42). Alternative, less-invasive approaches to transplantation are being actively investigated, such as hepatocyte transplantation therapies (13,17,48), human-tailored drug design (19,20), bioartificial liver (BAL) assist devices (6,9), and the development of transplantable tissue-engineered grafts (60). All of these approaches are dependent on viable human hepatocytes as the key functional component.

Since healthy human livers are prioritized for transplantation, primary human hepatocytes presently are derived from suboptimal sources. Disqualified donor livers produce limited quantities of cells that are highly variable in quality (4,5,25,58,59,68). Liver resections frequently result in acceptable viabilities but are constrained in yield and application (4,34). Nonhuman sources carry substantial risks aside from ethical concerns since extensive use of xenogeneic tissue poses issues of reduced clinical relevance, rejection, and transmission of infectious agents (21,69). Low function and potential risk of malignant transformation must be considered when using immortalized cell lines instead of primary hepatocytes, while ethical considerations persist with regard to the use of fetal liver cells (39), followed by an incomplete understanding of embryonic- and induced pluripotent stem cell-directed differentiation (22,24,47,53).

One approach to increase hepatocyte availability is to increase the yield from disqualified donor organs. By functioning as a therapeutic window in which to optimize organ viability, machine perfusion (MP) has the capacity to profoundly increase the availability and utility of donor

organs, particularly disqualified organs with reversible pathologies. The largest number of organs to benefit from MP derive from donors who have experienced cardiac death (DCD) since up to 90% are disqualified because ischemic durations have exceeded 30 min (4,14,16,18, 58,59,68). We and others have shown in preclinical models that as much as 60 min of warm ischemia can be recovered by MP to a transplantable state (2,35,50,54,55,57). Furthermore, we have demonstrated that the data procured during MP can diagnose the severity of ischemia, prognose the recovery to a transplantable state, and predict the likelihood of successful transplantation (44,45,61). Other pathologies can be similarly treated during MP, including the defatting of steatotic organs by increasing the catabolism of lipids and improving microcirculation with vasodilators (38,46,62); resecting or ablating liver tumors (7,43); inoculating donor organs against further viral damage posttransplantation (11,64); and preconditioning donor organs to better tolerate downstream ischemia (30). We have also demonstrated the role of MP in utilizing nonviable organs for the production of decellularized scaffolds that can then be repopulated with cells for the purposes of heterotopic cell transplantation (60).

To investigate MP as a means of optimizing livers for hepatocyte procurement, we developed and tested a novel, highly simplified system that integrates directly into existing cell isolation protocols. This paper describes the methods used and identifies a strong predictive correlation between the energetic state of the organ in perfusion and final cell yield. The consequences of MP are enhanced yields with functional characteristics of hepatocytes procured from ischemic livers that are comparable to fresh livers in cell suspension and plate cultures. The simplicity and effectiveness of this protocol bring MP a step closer to translation into clinical practice.

MATERIALS AND METHODS

Experimental Groups

The experimental groups were designed to evaluate the impact of machine perfusion on viable hepatocyte recovery from livers with different ischemic durations (Fig. 1). The positive control group for these experiments (Group 1: Fresh) comprised livers that underwent hepatocyte isolation. The negative control comprised livers exposed to an hour of warm ischemia (WI) prior to hepatocyte isolation (Group 2: WI). The two experimental groups comprised livers that experienced an hour of warm ischemia followed by 3 h of room temperature perfusion (Group 3: WI+3hrRT) and fresh livers that were perfusion-treated prior to digestion (Group 4: 3hrRT).

It should be noted that the routine isolation protocol was slightly modified to ensure procurement consistency between all groups: Specifically, in all rats, a hepatectomy was conducted prior to cannulation and perfusion.
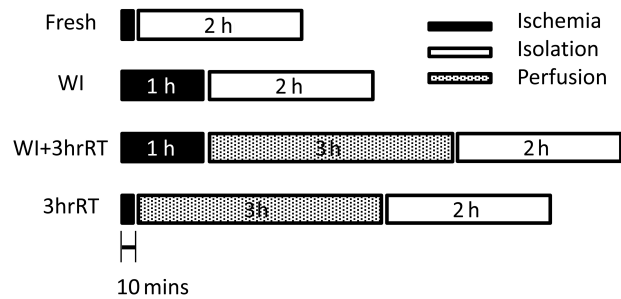

Figure 1. Experimental design: Fresh livers and 3hrRT livers experienced 10–12 min of ischemia (20°C). Warm ischemia (WI) and WI+3hrRT livers experienced 60 min of ischemia (34°C). Fresh and WI livers had hepatocytes isolated directly after ischemia while 3hrRT and WI+3hrRT livers were perfused for 3 h at room temperature prior to hepatocyte isolation.

For WI and WI+3hrRT livers, this allowed the organ to be placed in a temperature controlled chamber of saline and exposed to warm ischemia for exactly 1 h at near-body temperature (34°C) that reflected cooling of cadaveric tissue (57). In the cases of the Fresh and 3hrRT groups, hepatectomy exposed the livers to 10–12 min of room temperature ischemia (20–22°C) prior to perfusion that is normally avoided by perfusion in situ. Despite the introduction of ischemic time, there were no significant differences in hepatocyte yield or viability of Fresh cells compared to routine isolations (data not shown).

All experiments were conducted on female Lewis rats that weighed 160–180 g (Charles River Labs, Wilmington, MA, USA) and were kept in accordance with National Research Council guidelines. The Subcommittee on Research Animal Care, Committee on Research, Massachusetts General Hospital approved the experimental protocols.

Hepatectomy

Livers were procured and prepared as though for orthotopic liver transplantation according to the technique of Delrivière et al. (8). No pharmacological pretreatment such as heparin was administered to the donors. Briefly, using aseptic technique, animals were anesthetized with isoflurane (Forane, Deerfield, IL, USA) and a transverse abdominal incision was made. The intestines were retracted to expose the portal vein (PV), the common bile duct (CBD), and the inferior vena cava (IVC). The CBD was cannulated (12 cm×22 G Surflo polyethylene stent, Terumo, Somerset, NJ, USA) and the IVC freed from the right renal and adrenal veins. The portal vein (PV) was freed from the splenic and gastroduodenal veins. The right phrenic vein emptying into the suprahepatic vena cava (SHVC) was ligated. The hepatic artery was then ligated and the IVC clamped. Finally, the PV was clamped and the clock started for ischemic duration.

The diaphragm was opened, the SHVC was transected, and the liver was removed and weighed.

Fresh and 3hrRT livers were submerged into a room temperature saline bath (20–22°C) in order to cuff the PV and IVC using a 16 G and 14 G catheter (Terumo, Somerset, NJ, USA) respectively, for a cumulative ischemic duration of 10–12 min. WI and WI+3hrRT livers were submerged into a saline bath preset to 34°C, where they were similarly cuffed and retained for a cumulative ischemic duration of 60 min.

Ex Vivo Perfusion

Perfusate. The perfusate comprised 750 ml of phenol red-free Williams Medium E (Sigma Chemical, St. Louis, MO, USA) supplemented with 2 U/L insulin (28.85 units/mg Humulin, Eli Lily, Indianapolis, IN, USA), 100,000 U/L penicillin, 100 mg/L streptomycin sulfate (Gibco, Invitrogen, Grand Island, NY, USA), 0.292 g/L L-glutamine (Gibco), 10 mg/L hydrocortisone (Solu-Cortef, Pharmacia & Upjohn, Kalamazoo, MI, USA), and 1,000 U/L heparin (APP, Schaumberg, IL, USA).

Perfusion System. The circuit comprised a peristaltic pump (Masterflex L/S, Cole Parmer, Vernon Hills, IL, USA) and 14 G tubing (Masterflex® platinum-cured silicone tubing, Cole Parmer), which brought perfusate from a reservoir to a membrane oxygenating chamber (Radnoti, Monrovia, CA, USA), exposed to 95% O_2/5% CO_2. Perfusate then passed through a bubble trap (Radnoti) and into the PV (Fig. 2). 3hrRT and WI+3hrRT livers were suspended in perfusate by the PV cuff in a perfusion chamber (Radnoti) at room temperature (21±1°C). Effluent flowed freely from the IVC and SHVC into the chamber where it was then returned to the perfusate reservoir.

Samples. It was desirable to achieve in vivo flow rates of ~1.8 ml/min/g liver (27), but preference was given to attaining and sustaining an absolute pressure of 7–10 cm H_2O. Using a simple manometer (tubing attached at right angles to the inflow catheter), portal pressure P was estimated from the relationship that P is a function of the perfusate density ρ and acceleration due to gravity g and the height of the manometer h. The height of the manometer was recorded every 5 min for the first 20 min and then every half hour for the remainder of perfusion. Flow rates were initiated at 4 ml/min and then increased as portal pressure declined. Hepatic resistance R_{liver} was estimated using a hydraulic analog of Ohm's law where resistance is directly proportional to pressure P and inversely proportional to the flow rate Q (Equation 1):

$$R_{liver} = \frac{1}{v} \cdot \frac{gh}{Q} \qquad [1]$$

The constant of proportionality is the kinematic viscosity v of the perfusate formed by the ratio of the coefficient
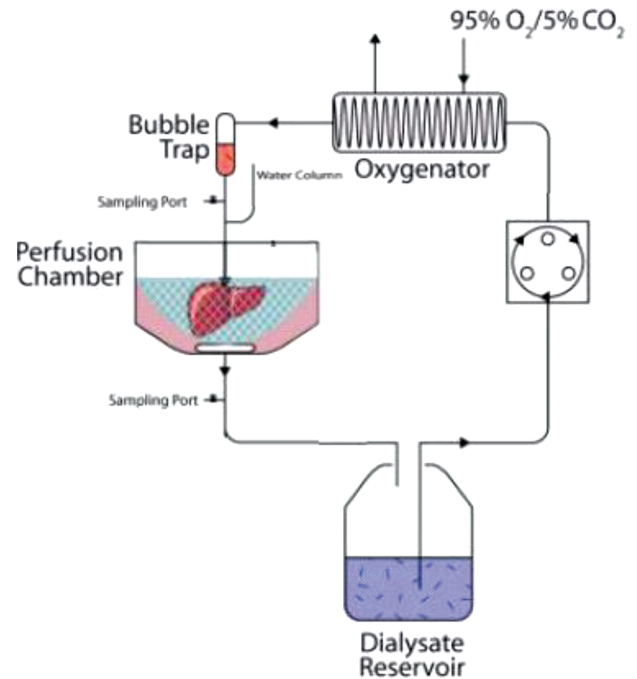

Figure 2. The machine perfusion system comprised a reservoir containing perfusate for organ recovery and optimization, followed by cell isolation solutions. The contents of the reservoir were pumped through an oxygenator exposed to 95% O_2 and 5% CO_2, prior to passing a bubble trap and entering the organ via the portal vein. Effluent from the infra- and suprahepatic vena cava was recirculated into the reservoir.

of viscosity μ to the perfusate density ρ. The kinematic viscosity v was estimated using the method of capillary flow as 4.53 cSt. Bile was collected in 1.6-ml Eppendorf tubes every hour and weighed. At $t=30$ min and every half hour thereafter, inflow and outflow partial oxygen tension pO_2 values in the perfusate were taken with a blood gas analyzer (Rapidlab, Chiron Diagnostics, Norwood, MA, USA). These data enabled calculation of oxygen uptake rate (OUR) as the difference between oxygen delivery rate (ODR $= 0.003 \times pO_{2,in} \times V$) and oxygen exit rate (OER $= 0.003 \times pO_{2,out} \times V$). At the same perfusion time points, 1.2 ml perfusate samples were collected from the reservoir and stored at −80°C for further analysis: Total protein was measured using the Bradford method of dye-binding solubilized protein (BioRad protein assay kit, Hercules, CA, USA). Commercially available kits were used for glucose (Stanbio 1075-825), urea (Stanbio proc. #0580, Boerne, TX, USA), lactate (Trinity Biotech proc. #735, Jamestown, NY, USA), alanine aminotransferase (ALT), and aspartate aminotransferase (AST) (Thermo Electron, Pittsburgh, PA, USA). Albumin was measured with an inverse competitive enzyme linked immunosorbent assay as described previously (10) using a polyclonal antibody to rat albumin (Cappel Laboratories

Inc., Cochraneville, PA, USA). The phosphate-buffered saline (PBS) supplemented with 0.05% (v/v) TWEEN® 20 for washing, citric acid monohydrate and sodium monohydrogen phosphate heptahydrate for the substrate buffer, and *o*-phenylenediamine for colorimetric evaluation at 490–650 nm were obtained from the same vendor (Sigma-Aldrich, St. Louis, MO, USA). All colorimetric (total protein, albumin, glucose, lactate, urea) and kinetic (ALT, AST) assays were evaluated with an xMark™ Microplate Absorbance Spectrophotometer #168-1150 (BioRad, Philadelphia, PA, USA).

Hepatocyte Isolation

The same MP system (Fig. 2) was used for both perfusion and cell isolation. At $t = 3$ h of perfusion, the circuit was opened at the point of the reservoir so that the efflux from the liver was captured in a new empty container, while the influx was switched to reservoirs containing isolation solutions preheated to 37°C. The MP system was heated to 37°C (Lauda-Brinkmann, Delran, NJ, USA). Nonperfused livers (Fresh and WI groups) were placed into the open, heated MP circuit upon completion of cuffing and exposure to ischemia, and hepatocyte isolation was initiated directly.

The isolation process comprised a two-step collagenase perfusion technique described by Seglen (51) and modified by Dunn et al. (10). All chemicals used in the isolation were from Sigma-Aldrich unless otherwise noted. Briefly, the first step comprised passing 350 ml of oxygenated Krebs Ringer Buffer (7.25 g sodium chloride, 1 g D-glucose, 2.1 g sodium bicarbonate, 0.5 g potassium chloride, 4.75 g HEPES per liter) and 0.0017 M ethylenediaminetetraacetic acid (KRB+EDTA) through the livers at a rate of 17 ml/min for a total of 20 min. The second step comprised passing prewarmed collagenase solution containing 130 mg type IV collagen (C5138-1G) in 150 ml KRB and 9 ml of 125 mM $CaCl_2$ through the liver until successful digestion was observed. The livers were then moved to a sterile hood on ice where approximately 10 ml of sterile, cold KRB were added. The liver capsule was gently broken to release the cells, which were then passed through a 250-μm filter followed by a 60-μm filter. The suspension was divided into 50 ml conical tubes and centrifuged at low speed (15–21g, 4°C, no brake, 5 min) (Beckman GS-6, Brea, CA, USA). The supernatant was aspirated and the pellet resuspended with 10 ml KRB. An initial count of cell number and viability was performed using a trypan blue (TB) exclusion assay. A volume of 24 ml of cold Percoll® solution (9 parts Percoll® to 1 part 1.5 M NaCl, pH 5–5.5) was used for every 25 ml of cell suspension. Cells were added at a concentration of 5 million cells/ml and inverted several times before being centrifuged (49–58g, 4°C, no brake, 10 min) (Beckman GS-6). The buffy coat and supernatant

were discarded, and the cell pellet was resuspended to 10 ml in Dulbecco's modified Eagle's medium (DMEM) with 10% fetal bovine serum (FBS), 100,000 u/L penicillin and 100 mg/L streptomycin sulfate. A final count was then performed.

Cell Suspension

Cells were diluted to 1 million/ml in Williams Medium E and aliquoted into 1.6 ml microcentrifuge tubes. Four separate vials were used for each assay, except for TB exclusion where time permitted only 2 (counted simultaneously by BEU and MAG or ML). A total of 34 vials (34 million cells per liver) were aliquoted for cell suspension studies per liver. As WI livers did not provide an adequate number of cells for all assays, priority was given to evaluating cell viability (TB exclusion), ALT/AST release, and metabolite synthesis. The tubes for all assays were subsequently rotated at slow speeds in a 37°C incubator, except for light-blocked vials for cytochrome P450 (CYP450) activity, which were allowed to settle between readings and manually agitated after each reading.

Viability. Two vials were counted hourly using TB exclusion as described earlier.

Mitochondrial Activity. Cells for the conversion of the yellow tetrazole MTT (3-(4,5-dimethylthiazol-2-yl)-2,5-diphenyltetrazolium bromide) into purple formazan were taken at the first and sixth hour of the cell suspension studies. Fifty microliters (approximately 50,000 cells) were pipet-transferred from four vials per group into four wells on a 96-well plate and diluted with 50 μl of Williams Medium E. One vial of MTT was thawed (Biotium, Inc., Hayward, CA, USA) and 10 μl added to each well. Samples were mixed gently while incubating at 37°C for 1 h and protected from light. The plates were then spun at 800 rpm (Beckman GS-6), the supernatant was aspirated, and 200 μl of dimethyl sulfoxide (Sigma) was added to dissolve the formazan. Absorbance was read at OD_{570}–OD_{630}.

ALT and AST. At hourly time points starting at $t = 0$ h, 15 μl from each of four vials was pipetted into a 96-well plate on ice. A positive control for ALT and AST was prepared at $t = 6$ h by lysing the remaining cells with Triton X-100, diluted to 1% concentration with a volume of the cell suspension followed by rapid up-and-down pipetting. The lysed suspension was diluted 1:4 with 1× phosphate-buffered saline (PBS; lab stock) and 15 μl from each vial added to the 96-well plate. One hundred fifty microliters of commercially available reagent (TR71121 and 7200-006, Thermo Electron) at room temperature was pipetted into all the wells initiating a kinetic endpoint assay to determine enzyme activity per minute. ALT and AST activities were expressed as a percentage of the maximum activity observed in the positive controls.

Glucose, Albumin, and Urea. Four vials were incubated for 6 h, after which they were centrifuged for 5 min at $3,000 \times g$ (5415C, Eppendorf, Hauppauge, NY, USA), and the supernatant was stored at $-80°C$. The supernatant was tested for glucose, albumin, and urea in the hourly analysis of perfusate as aforementioned. At baseline, Williams Medium E contains 2 g/L glucose, 0 mM of urea, and 0 μg/ml albumin.

CYP450 Activity. Cells to test four CYP450 enzymes associated with drug and steroid metabolism were suspended in 4×4 light-protected vials per group. Thirteen microliters of 6 mM stock solution of the competitive oxidoreductase inhibitor 3,3′-methylene-bis(4-hydroxy-coumarin) (M1390, Sigma) were added to each vial and allowed to incubate for 20 min to prevent diaphorase-mediated metabolism of resorufin. Then 10 μl of 1 mM solutions of benzyloxyresorufin, pentoxyresorufin, ethoxyresorufin, and methoxyresorufin (Invitrogen, Carslbad, CA, USA) were added as substrates for the enzymes CYP2B2, CYP2B1, CYP1A1, and CYP1A2, respectively. The vials were inverted several times, and a 50-μl sample was taken and placed into a light-protected 96-well plate on ice, marking $t = 0$ min of the assay. Samples were taken again at 10, 20, 30, and 40 min. A standard was prepared by serial dilution of 1,000 nM resorufin (Invitrogen). Samples and standards were read with a fluorescence plate reader (Ex530, Em590, FMAX Fluorescence Microplate Reader, Molecular Devices, Downington, PA, USA) and recorded as rates of resorufin production per million cells.

qRT-PCR. RNA was extracted from approximately 1 million freshly isolated cells using Nucleospin RNA II total RNA extraction kit (Clontech Laboratories, Mountain View, CA, USA). Total RNA quality was assessed by spectroscopy and converted to cDNA using the Invitrogen SuperScript III Platinum Two-Step RT-PCR Kit following the manufacturer's instructions. cDNA was analyzed by qPCR using the Stratagene mx3005P instrument. A melting curve was used to confirm the specificity of each primer pair. Each sample was run in triplicate to exclude outliers. Samples were evaluated for select Phase I and II genes (Table 1). Gene expression was analyzed using the $\Delta\Delta CT$ method, using β-actin as the normalizer gene.

Plate Culture

Cells were plated in triplicate in standard six-well plates using a double-layer collagen gel sandwich plate culture (10) with phenol red-free Williams E as the culture medium. In the viability, mitochondrial activity, and CYP450 activity assays, three wells were devoted to each of the four time points (days 5, 7, 10, and 14), requiring 64 million cells per liver. Glucose, albumin, and urea assays were conducted on medium aspirated daily from

Table 1. List of Genes Used in Quantitative RT-PCR

Description	Symbol	Primer
Phase I enzyme	cyp1a2L	cccacacctatctctgacaa
	cyp1a2R	ggttgaaagtcatgctcttg
	cyp2b3L	gagcgctttgactacagaga
	cyp2b3R	gaactccgtgtagtggttca
	cyp3a2L	gcacactctcctttgtcttg
	cyp3a2R	gggtcatgatgaagagcata
	cyp2c11L	ctttatgccattctcagcag
	cyp2c11R	agacaggaccctcagaagag
Phase II enzyme	ugt1a1L	tctgcctgctgtgtacttct
	ugt1a1R	caaagtcgtttctcatcagc
	nnmtL	ggagaaggaggagaagttga
	nnmtR	tctgttccccaatcatgtag
Normalization	ck18L	gagtaccacggtagtcacca
	ck18R	caagcttgaccttgatgttc
Drug transporter	ntcpL	tcgtcatgacaccacactta
	ntcpR	tctcatagcaccggaagata
	oatpL	gtggtgattggtattggatg
	oatpR	aagggcacaataggagtttc
	oct1L	ggagctgaactacactgtgc
	oct1R	ccaggttaaactcagtgacg
Apical surface drug transporter	Slc10a1L	tcgtcatgacaccacactta
	Slc10a1R	tctcatagcaccggaagata
	mdr1L	gggtctaggcttgctgttat
	mdr1R	caagctctgggcatacatag
Basal surface drug transporter	mrp3L	ctcagtccttctttgacacg
	mrp3R	gctaacggattccagtctct
Positive control	β-actinL	ctgaagtaccccattgaaca
	β-actinR	gtacgaccagaggcatacag

the same three wells (3 million cells per liver). A total of 70 million hepatocytes per liver were reserved for plate culture studies. Attempts to plate culture cells from WI livers were made; however, the cell yield was too low to enable a complete set of data to be procured from each liver and the cultures themselves did not reach confluence and frequently failed by the 8th or 9th day of culture. As a consequence, phase contrast images of WI cells were procured on day 7 to visualize culture quality (Axiovert 200 inverted microscope, Carl Zeiss, Thornwood, NY, USA), but this group was otherwise excluded from plate culture evaluation.

Viability. The double stain Hoechst 33452 and Ethidium homodimer-1 (Invitrogen) was used to detect all nuclei and dead nuclei, respectively, on days 5, 7, 10, and 14 of cell culture. Briefly, 10 μl of a 1-mM solution of Ethidium homodimer-1 and 5 μl of Hoechst 33452 were added to 5 ml of $1 \times PBS$. Medium from the cells was aspirated and 1 ml of the dye–PBS solution was added to each well. Cells were incubated at 37°C for 10–15 min before imaging (Axiovert 200 inverted microscope, Carl Zeiss). Images were taken at 35 distinct locations within each

well for each dye and overlaid on corresponding phase-contrast images. Stained cell nuclei were subsequently counted using CellProfiler (Broad Institute, Cambridge, MA, USA), and the fraction of live cells was determined as the difference between total nuclei and dead nuclei.

Mitochondrial Activity. One hundred microliters of MTT were added to each well and incubated for 1 h at 37°C. The medium+MTT was subsequently aspirated from the wells and 1 ml of 6 mg/ml collagenase (C5138-1G, Sigma) was added and incubated at 37°C for 15 min and pipetted rigorously to dissolve all collagen. One milliliter of dimethyl sulfoxide (Sigma) was then added, and the contents rigorously pipetted up and down to dissolve the formazan present. Two hundred and fifty-microliter samples were subsequently placed in triplicate on a 96-well plate (3 wells×3 samples), and absorbance was read at OD_{570}–OD_{630}.

CYP450 Activity. The isoenzymes CYP4502B2, CYP4502B1, CYP4501A1, and CYP4501A2 previously evaluated in cell suspension were also evaluated in triplicate in plate culture. At 48 h before the assay, medium from the cells was aspirated and replaced with 1 ml/well of a 2-μM solution of 3-methylcholanthrene (213942, Sigma) to induce CYP450 enzymes at 37°C for 2 days. After 48 h, the medium was aspirated, washed with 1 ml of warm Earle's Balanced Salt Solution (EBSS, Sigma), and then after 15 min, replaced with 1 ml of the 5-μM substrate and 80-μM 3,3′-methylene-bis(4-hydroxycoumarin) solution in warm EBSS. Fifty microliters of medium was subsequently removed at $t=5$, 15, 25, and 35 min and placed in a 96-well plate protected from light. A standard was prepared by serial dilution of 1,000 nM resorufin. Samples and standards were read with a fluorescence plate reader (Ex530, Em590, FMAX Fluorescence Microplate Reader, Molecular Devices, Downington, PA, USA) and recorded as rates of resorufin production per million cells.

Glucose, Albumin, Urea. Three wells per liver were maintained until day 14. Media taken from daily cell washes were preserved for metabolic analysis using the aforementioned assays in the hourly analysis of perfusate.

Tissue Biopsies

Three livers from each group were used to procure tissue biopsies instead of undergoing cell isolation as an endpoint.

Adenosine Triphosphate (ATP). Samples taken from each of the lobes of the liver were snap-frozen in liquid nitrogen. ATP was measured using the ApoSENSOR™ ATP Luminescence Assay Kit (Biovision, Mountain View, CA, USA) modified to evaluate tissue biopsies. Briefly, the tissue was homogenized under liquid nitrogen and resuspended in 500 μl of the assay nucleotide releasing buffer. Samples were spun down at 16,000 rpm for 2 min. One hundred microliters of sample supernatant was pipetted into a cuvette to which 1 μl of ATP monitoring enzyme was added. The resulting luminescence was rapidly assayed in a luminometer (FB12 Luminometer, Titertek Berthold, AL, USA). Data were evaluated against an ATP standard and normalized to the total protein present in the sample supernatant using the Bradford stain (BioRad protein assay kit, Hercules, CA, USA).

Light Microscopy. Tissue remaining from the livers used for ATP analysis was carefully sliced, fixed in 10% formalin solution, embedded in paraffin, sectioned, and stained with periodic acid-Schiff (PAS stain) for glycogen, hemotoxylin and eosin for general hepatic structure, and terminal deoxynucleotidyl transferase dUTP nick end labeling (TUNEL) for apoptosis. Tissue staining was conducted externally by the Specialized Histopathology Services at the Massachusetts General Hospital (Boston, MA, USA).

Statistical Analyses

All analyses were performed in MATLAB 2010b (ver 7.11.0584, 64 bit; MathWorks, Inc., Natick, MA, USA). For results in each subfigure with quantitative data, the differences between groups (Fresh, 3hrRT, WI+3hrRT, WI) and any other factors (Percoll, CYP450s, etc.) were analyzed via N-way ANOVA. Multiple group comparisons were performed by function MULTCOMPARE in MATLAB with Tukey–Kramer correction for multiple comparisons. Statistical significance limit was set at $p<0.05$. Where applicable outliers (>3 standard deviations from the mean) were excluded from the analyses.

For correlation analysis between ATP and cell yield Pearson's linear correlation method was used via function CORR in MATLAB, which produced a p value for statistical evaluation of the correlation.

RESULTS

Simple Machine Perfusion Significantly Enhances Hepatocyte Yields

After 3 h of room temperature machine perfusion, WI+3hrRT livers yielded 39±11 million hepatocytes/g liver with 92±2.7% viability (Fig. 3A), a significant increase ($p<10^{-5}$) from the 1.9±0.8 million hepatocytes/g liver with 88±5.0% viability procured from nonperfused WI livers. Fresh livers produced 32±8.6 million hepatocytes/g liver with 92±3.6% viability, which was not significantly less than WI+3hrRT ($p=0.57$). 3hrRT livers produced 45±12 million hepatocytes/g liver tissue with 92±3.6% viability, 40% more cells than Fresh livers ($p=0.039$) but not significantly more than WI+3hrRT livers ($p=0.35$). With the exception of WI livers, which had a 41±7.6% viability pre-Percoll treatment and retained
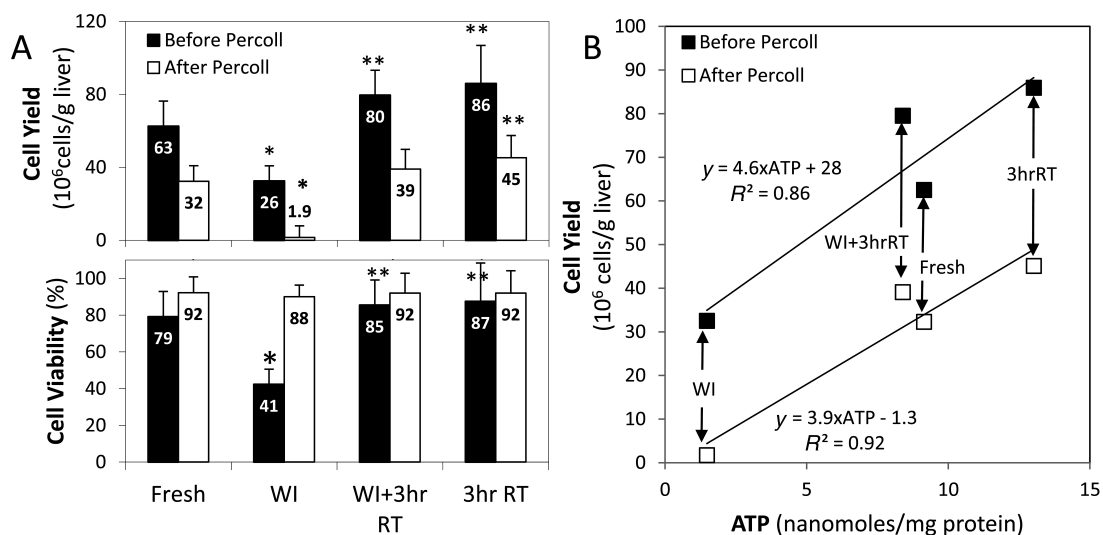
Figure 3. Ischemia and machine perfusion significantly impact cell yield, viability, and adenosine triphosphate (ATP) content. (A) Cell yields, normalized to wet liver weights, show that perfusion-treated WI livers increase their yield of viable cells 25-fold from untreated WI livers. In addition, perfusion of nonischemic livers increases cell yields by 40%. (B) Biopsy ATP, normalized to total protein content, is directly correlated to hepatocyte yields both before and after Percoll, serving as a useful indicator of machine perfusion recovery. *Significantly different than Fresh ($p < 0.05$). **Significantly different than 3hrRT ($p < 0.05$). Data shown are means ± SD.

only 4 ± 2% of the initial cell yield post-Percoll, all other groups had initial viabilities of 79–87% and retained 49–53% of the cells post-Percoll. The differences in cell viability after Percoll were not statistically different ($p > 0.73$).

Liver ATP Content Predicts Cell Yields

Since ATP depletion occurs rapidly upon the inception of warm ischemia, ATP content in WI liver biopsies was predictably lowest ($p < 10^{-4}$ for all comparisons) (Fig. 3B). Perfusion treatment increased WI+3hrRT liver ATP to levels comparable with Fresh livers ($p = 0.50$). 3hrRT livers were found to have a significantly higher ATP yield than Fresh livers ($p = 0.004$). The relationship between ATP and final cell yield was linear by Pearson's correlation 0.96 ($p = 0.04$), enabling quantitative prediction of liver recovery as a result of perfusion.

Hepatocyte Performance in Short-Term Suspension Cultures

Isolated hepatocytes were evaluated over a 6-h period in suspension culture (10^6 cells/vial) to determine their functional capacity and longevity. Unlike the other groups, 3hrRT cells showed no significant decline in viability over time with Trypan Blue exclusion (Fig. 4A); the results were confirmed by similar trends of formazan production (data not shown). Hepatocyte injury in 3hrRT, WI+3hrRT, and WI groups, monitored by aspartate (AST) and alanine (ALT) aminotransferase release, did not increase throughout suspension culture and was not significantly different from Fresh cells (Fig. 4B). Metabolically, WI cells

produced significantly less glucose ($p = 0.0018$), albumin ($p = 0.003$), and urea ($p = 0.0019$) than any of the other groups. By contrast, WI+3hrRT livers showed recovery of all metabolic functions with the exception of albumin production, which was not significantly different from WI cells ($p = 0.17$) (Fig. 4C). The capacity for drug metabolism was evaluated by the resorufin production of four cytochrome P450 enzymes (Fig. 4D) (WI cell analyses were not completed due to limited number of cells available for analysis). CYP450 activities had no statistical differences, except CYP4502B1 of 3hrRT cells showed a twofold increase in activity ($p < 10^{-4}$). Furthermore, expression profiles of liver-specific CYP450 and phase II genes (Table 1) from cells at $t = 0$ h of suspension were not significantly different between perfused and Fresh isolated cells ($p = 0.11$, data not shown).

Hepatocyte Performance in Long-Term Plate Cultures

Using the collagen sandwich technique, isolated hepatocytes were evaluated over a period of 2 weeks. WI cells, plated and evaluated with phase contrast microscopy at day 7, showed poor morphology with little confluent organization and noticeable cell debris, suggesting poor adherence and significant cell death (Fig. 5A); further evaluation of WI cells was not conducted since there were too few cells to conduct all the proposed assays and the cultures failed. WI+3hrRT liver cells by contrast were confluent, hexagonal in shape, and nonsteatotic, similar in appearance to Fresh cells. Both perfusion groups had higher viabilities (Fig. 5B) compared to the Fresh group ($p < 0.001$) throughout culture; viability was constant
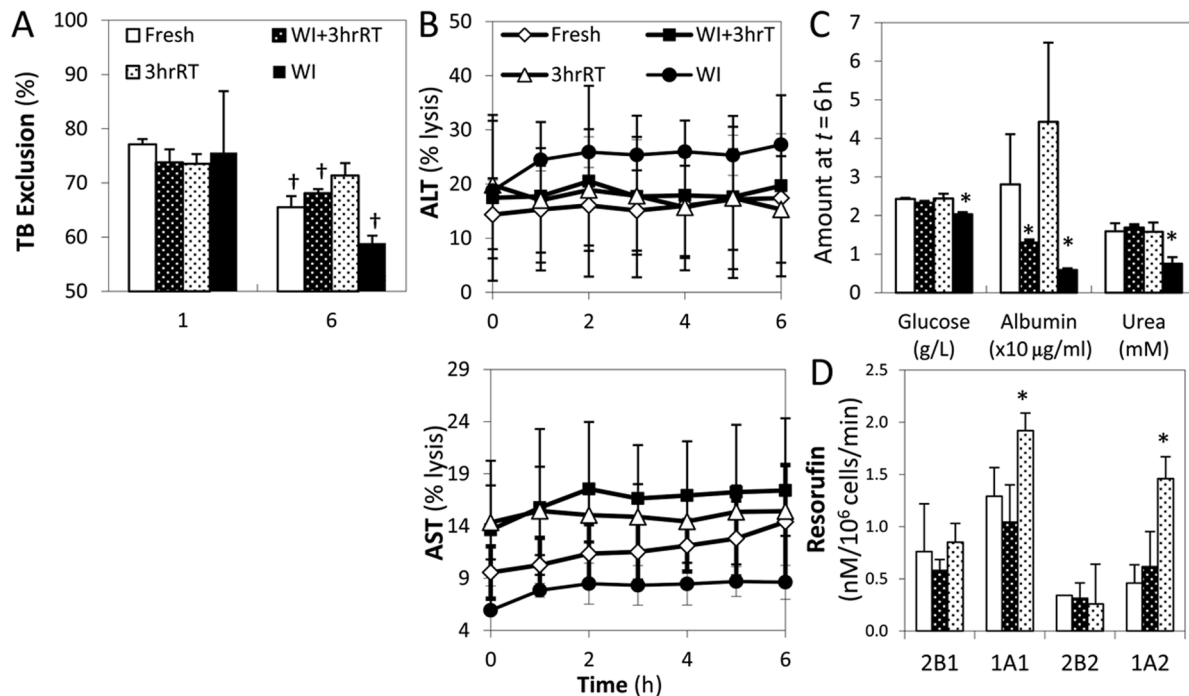
Figure 4. Evaluation of hepatocyte performance in suspension culture. (A) Viability of cells is evaluated by the percent of cells with intact membranes able to exclude Trypan Blue (TB). (B) Cell damage is measured by cellular release of alanine aminotransferase (ALT) and aspartate aminotransferase (AST) enzymes over time. (C) Metabolic activity is measured by the production of glucose, albumin, and urea. (D) Cytochrome p450 (CYP450) activity is measured by the dealkylation of pentoxy resorufin (2B1), ethoxy resorufin (1A1), benzyloxy resorufin (2B2), and methoxy resorufin (1A2) to resorufin. *Significantly different than Fresh ($p < 0.05$). †Significantly different than suspension at 1 h ($p < 0.05$). All data shown are means ± SD.

over time in all groups ($p = 0.63$). MTT activity in the WI+3hrRT group was lower than Fresh and 3hrRT groups initially ($p < 0.05$), but by day 7 was similar in value to the other groups. CYP450 activity did not differ significantly across groups or over time ($p > 0.05$ and $p > 0.11$ for all cases, respectively) (Fig. 5C). The average daily production of albumin by WI+3hrRT cells was significantly less than Fresh and 3hrRT cells ($p < 10^{-5}$ in both cases), while the rate at which production increased daily was similar across groups (Fig. 5D). 3hrRT cells produced significantly more urea per day than WI+3hrRT or Fresh cells ($p < 10^{-4}$ in both cases); after day 7 the daily rate of production was generally constant across groups (Fig. 5E). Glucose metabolism was stable and similar between groups over the 2 weeks of culture (Fig. 5F).

Liver Performance in Machine Perfusion

Distinctions between 3hrRT and WI+3hrRT livers in MP appeared at the level of the microvasculature. At the initiation of MP, using flow rates that were comparable between 3hrRT and WI+3hrRT livers (Fig. 6A), blood, debris, and clots were cleared from the livers, measured as total protein release (Fig. 6B). WI+3hrRT livers

dispelled only 90% as much total protein as 3hrRT livers and had trends of higher portal pressures and hepatic resistances (Fig. 6B–D). The removal of debris was particularly prominent in WI+3hrRT livers, seen as a receding edge of clotted blood toward the periphery of each liver lobe, which cleared over the course of 20 min leaving the organ ultimately homogeneous in appearance (Fig. 7A). In both groups, protein release subsided within 20 min of perfusion, which corresponded to an initial steep decline in hepatic resistance (Fig. 7B). Hepatic resistance continued to decline during perfusion, despite a cessation of protein release; however, 3hrRT livers sustained a 10% lower resistance than in WI+3hrRT livers at the end of perfusion. Room for further perfusion optimization in WI livers was observed with multiple parameters: Glycogen content, which was markedly reduced in periportal hepatocytes after an hour of warm ischemia, was incompletely recovered in WI+3hrRT livers at the end of perfusion (Fig. 7C). WI+3hrRT livers consumed 10% less oxygen compared to 3hrRT livers throughout perfusion (Fig. 7D), had delayed production of bile (Fig. 7E), and released more ALT and AST (Fig. 7F). Furthermore, the relationship between perfusion flow rates and cell
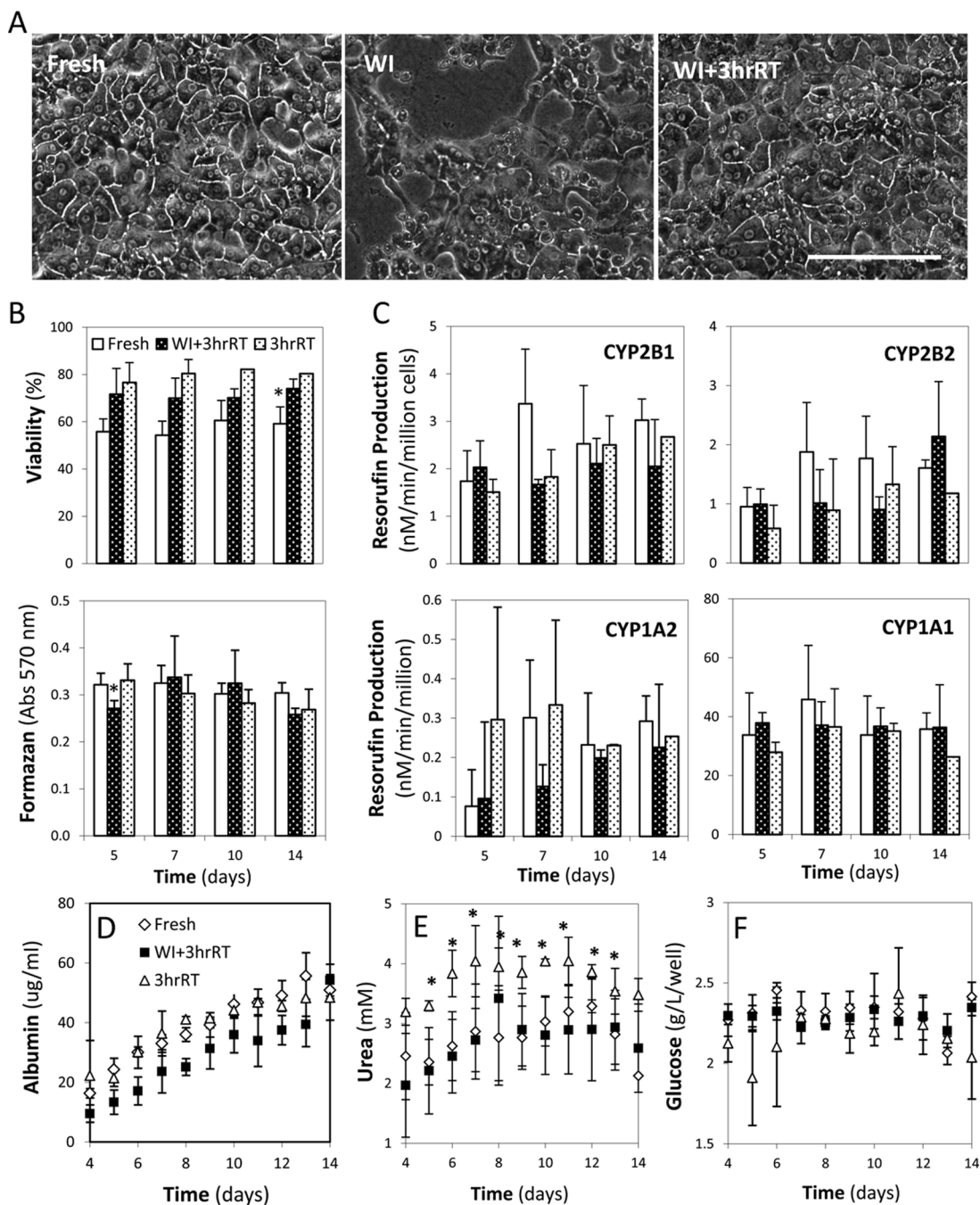
Figure 5. Evaluation of hepatocyte performance in double-layer collagen gel sandwich plate culture: (A) Phase contrast images compare Fresh, WI, and WI+3hrRT livers (20×) at 7 days of culture. (B) Cell viability is quantified both by using Hoechst 33452/Ethidium homodimer-1 double stain and mitochondrial activity measured by MTT reduction to formazan. (C) CYP450 isoenzyme activity is evaluated at days 5, 7, 10, and 14 of culture. (D–F) Albumin, urea, and glucose production is measured daily. *Significantly different than Fresh ($p < 0.05$). All data shown are means ± SD. Scale bar: 200 μm.

yield was nonlinear in WI+3hrRT liver groups while perfusion flow rates correlated directly with cell yields from 3hrRT livers (Fig. 7G).

WI+3hrRT and 3hrRT livers did not have significantly different glucose levels, which were stable, or rates of urea, lactate, and albumin production. Microscopically, structural integrity of the livers was preserved and there were no remarkable differences in H&E images and TUNEL, which were negative for necrosis and apoptosis respectively (data not shown).
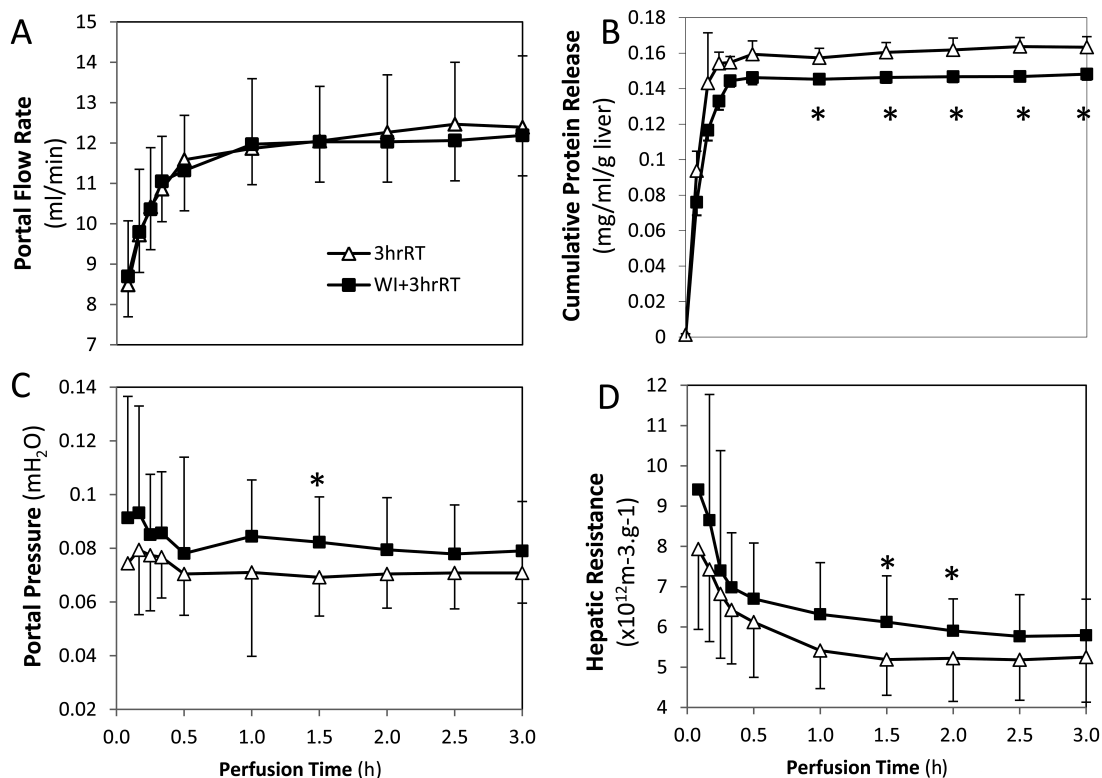
Figure 6. Machine perfusion sets the flow rate into the portal vein, which impacts portal pressure, hepatic resistance, and the rate of protein-containing material released from the liver. (A) Perfusion flow rates of 3hrRT and WI+3hrRT livers are similar. (B) Cumulative protein release during perfusion is significantly less in WI+3hrRT livers than in 3hrRT livers ($p<0.05$). (C) Portal pressure tends to be higher in WI+3hrRT livers. (D) Hepatic resistance declines during perfusion but remains higher in WI+3hrRT livers than in 3hrRT. Data are expressed as mean ± SD.

DISCUSSION

The shortage of viable donor organs is critically limiting not only transplantation but also the development of new, less-invasive hepatocyte-dependent therapies such as cell transplantation and bioartificial liver assist devices. Yet thousands of donor organs are discarded every year because of excessive ischemia. We demonstrate in rat livers exposed to an hour of warm ischemia that a 25-fold increase in high-quality hepatocytes is possible using simple machine perfusion. MP efficacy is also apparent in the dramatic difference in cell function in suspension and plate culture compared to untreated ischemic cells. While untreated ischemic cells have little metabolic functional capacity and are incapable of surviving over long periods of culture, perfusion-recovered cells appear to have no distinguishing differences compared to Fresh cells based on the particular functions tested here. Translation of these findings to human donor livers may enable more donor organs to be considered for procurement, in addition to increasing the yield of viable hepatocytes per organ.

Our results demonstrate that one mechanism by which perfusion operates is to recover cellular ATP levels.

Since failure to recover ATP initiates a cascade of destructive events that results in cell death and subsequently graft failure (28,33,65), it is not surprising that there is a direct correlation between ATP and the number of viable cells in the organ. This useful correlation has also been observed in cold ischemic organs, where the rate of decline in viable cell content over time is proportional to the remaining biopsy ATP content (3). Kamiike et al., who demonstrated similarity across species in cellular ATP decline during warm ischemia, also showed that ATP recovery on reperfusion is slower as ischemic duration increases (28,29). MP provides the time required to recover ATP values, and hence cellular integrity, in a manner that significantly minimizes ischemia reperfusion injury (54), since this is likely to play a significant role in the inability to successfully transplant ischemic organs (37,52,65). ATP recovery during MP is therefore a valuable metric of organ recovery. However, it is impractical to measure during perfusion and repeated biopsies severely damage the organ; therefore, alternative data-mining approaches using online metrics of organ performance are desirable (44,45).
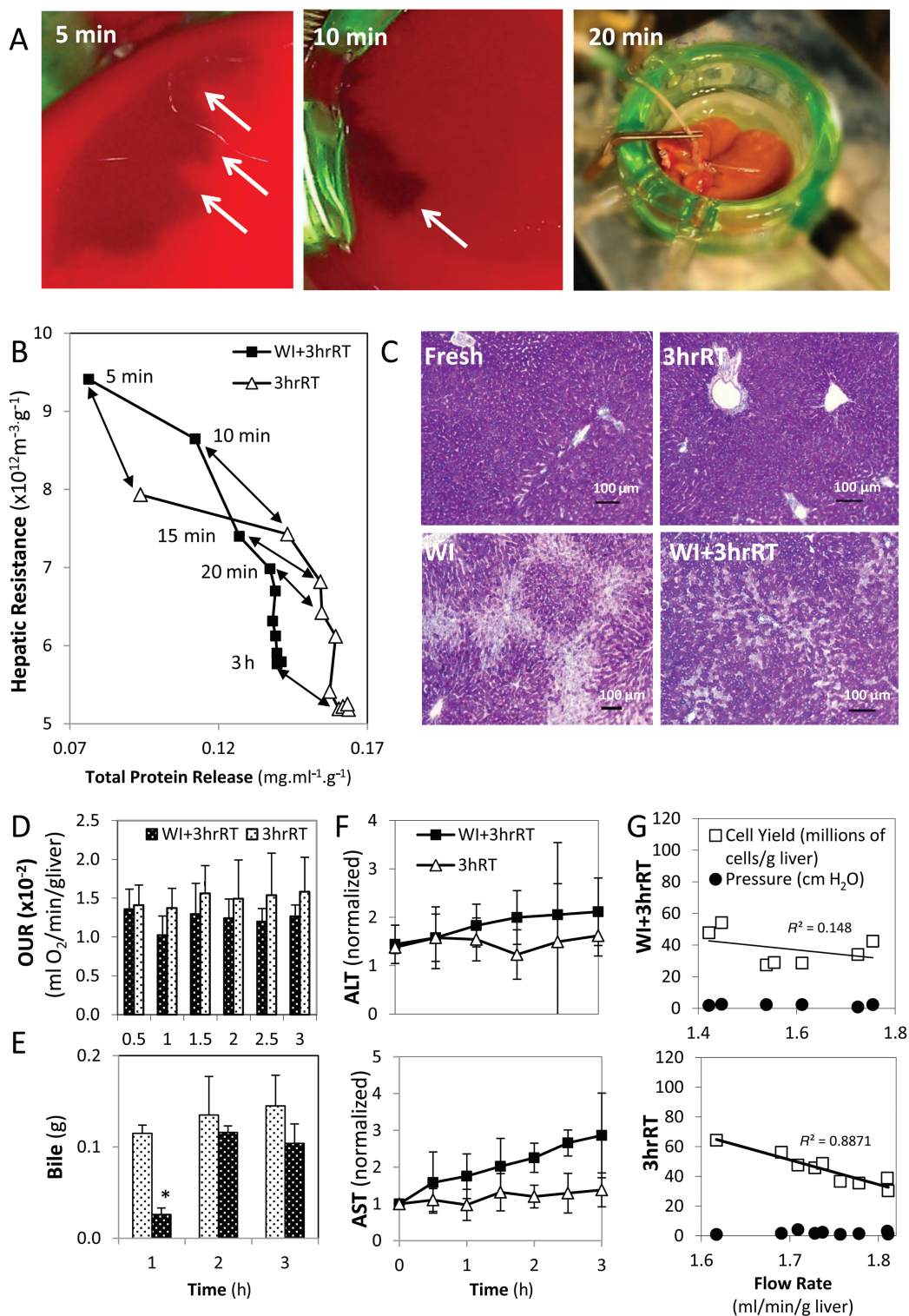
Figure 7. 3hrRT and WI+3hrRT livers differ in the quality of perfusion through the hepatic microvasculature. (A) Clotted blood and other cellular debris (arrows) are washed out of WI+3hrRT livers within the first 20 min of perfusion. (B) Hepatic resistance declines as protein-containing material is released from the vasculature and vasodilation occurs. (C) Glycogen is heavily depleted in the periportal spaces of WI livers, but it is mostly recovered after 3 h of perfusion. (D) WI+3hrRT livers consume 10% less oxygen than 3hrRT livers throughout perfusion. OUR, oxygen uptake rate. (E) Bile production is recovered in WI+3hrRT livers after the first hour of perfusion. (F) ALT and AST release occur gradually throughout perfusion in WI+3hrRT livers. (G) Impaired perfusion in the microvasculature obscures the correlation between lower flow rates and higher cell yields in WI+3hrRT livers. Data shown are means±SD.

Another mechanism by which machine perfusion operates is evident through the most surprising finding in this study, which is the significantly increased (1.4-fold) recovery of hepatocytes from perfused Fresh organs. This result appears to be associated with perfusion-induced changes in the microvasculature. Perfusion through the liver is enhanced by clearance of debris within the first 20 min of MP, correlating with a decline in hepatic resistance (Fig. 7B). This is also observed during the first flushing step in routine hepatocyte isolations. Unique to MP, however, is the continued decline in hepatic resistance that occurs over the next 2 h. The reduced resistance is most likely due to vasodilatation of the vasculature (67), providing superior access to hepatocytes upon initiation of the isolation process. Consequently, though WI+3hrRT livers were recovered to physiological levels of ATP and Fresh cell yields, they most likely could have benefited from longer perfusion durations to further diminish hepatic resistance and optimally recover ATP and glycogen stores. Superior to extending perfusion duration, future additions of vasodilators to the perfusate may enable more rapid declines in hepatic resistance and greater release of occlusive cellular matter in the vasculature early in perfusion to maximize perfusion quality and minimize cell damage, potentially recovering organs with even more severe ischemic damage.

Our particular MP method has been designed with emphasis on simplicity and ease of integration into existing hepatocyte isolation protocols. Since the methodology simply adds a perfusion step prior to the initiation of the digestion process, it can be readily applied across species and modified to accommodate resected liver segments. An important consideration in translating this method to human-sized organs, which are two orders of magnitude larger than rat livers, is that direct scale up of perfusate volume (750 ml:75 L) is impractical. While the perfusate volume in the rat model functions as a relatively stable metabolite reservoir, larger livers will require detailed analysis of metabolite fluctuations during perfusion to enable supplementation with necessary nutrients and minimize toxin accumulation. Hastening the recovery process is highly desirable since it will reduce the effort required to manage the perfusate content, as well as reduce the overall duration of the process. Perfusate additions such as vasodilators and more readily-available ATP precursors such as adenosine may work synchronously to achieve optimal recovery earlier. Livers larger than the rat model can be perfused through both portal and arterial vasculature. The quality of perfusion may be enhanced by dual vessel perfusion, both improving hepatocyte recovery and facilitating preservation of the biliary tree (41), but at the cost of adding complexity to the isolation system. Human donor livers are likely to have a range of pathological conditions that negatively impact hepatocyte recovery. Further research is required to expand on the ability to diagnose disease severity during MP (44) and make use of tailored perfusates to treat specific pathologies (38,62).

The experimental evidence supporting machine perfusion-preservation of donor livers is extensive (66). Animal models conclusively illustrate the value of MP in optimizing the quality (44,45) and maximizing the use of donor organs for transplantation (2,57), isolated cell yields, and decellularized scaffold production (60). Translation of MP to the clinic is under active investigation (15,23) but a determining factor of its success will be the ease with which it can be integrated into the current organ procurement process. MP at ambient temperatures is a valuable simplifying step towards this requirement. In addition to removing the need for stringent temperature regulation, room temperature MP can use asanguineous, quantified perfusates (12,40). This is a significant benefit over heated normothermic perfusions (37°C), which require oxygen carriers that are typically blood-based to support high metabolic activity (50,56). Furthermore, room temperatures are high enough to enable metabolic recovery, but low enough to inactivate destructive enzymes and reduce the rate of cellular degradation (1,63). Compared to severely hypothermic MP (4°C) (35,36), room temperatures also minimize cold-induced damage by avoiding the transition temperature of plasma lipids (26) and decreasing sensitivity to reperfusion injury, which endothelial cells are particularly prone to (31,49,63). Enhanced preservation of the endothelium, and consequently the integrity of the microvasculature, is highly desirable since it means better microcirculation in the organ. As a consequence, access to and recovery of hepatocytes is improved and, depending on the use of the organ, there will be better cell isolation or transplantation outcomes. Overall, the structural integrity and functional capacity of the various cell types within the organ appear to be upheld by room temperature MP. We demonstrate this here by well-preserved functional hepatic architecture that homogeneously exposes hepatocytes to perfusate for glycogen recovery (Fig. 7C) and elsewhere by long-term follow-up posttransplantation (2,54). While substantial research has yet to be done to translate these results to the clinic, this technology has immediate application in enhancing viable hepatocyte yields and providing data necessary to develop a quantitative index of the organ recovery process.

In summary, simple machine perfusion significantly increases the yield of viable hepatocytes from rat livers with negligible to severe ischemic stress. Furthermore, MP visibly enhances the functional capacity and longevity of ischemic hepatocytes under culture conditions. Machine perfusion has the capacity to maximize donor organ viability and recover the use of a large number of donor organs that are otherwise discarded.

REFERENCES

1. Ar'Rajab, A.; Ahren, B.; Nilsson, A. Temperature dependent phospholipid degradation in the rat liver during preservation for transplantation. Transplantation 57(8):1153–1160; 1994.

2. Berendsen, T. A.; Bruinsma, B. G.; Lee, J.; D'Andrea, V.; Liu, Q.; Izamis, M. L.; Uygun, K.; Yarmush, M. L. A simplified subnormothermic machine perfusion model restores ischemically damaged liver grafts in a rat model of orthotopic liver transplantation. Tranplant. Res. 1:6; 2012.

3. Berendsen, T. A.; Izamis, M. L.; Xu, H.; Liu, Q.; Hertl, M.; Berthiaume, F.; Yarmush, M. L.; Uygun, K. Hepatocyte viability and adenosine triphosphate content decrease linearly over time during conventional cold storage of rat liver grafts. Transplant. Proc. 43(5):1484–1488; 2011.

4. Bhogal, R. H.; Hodson, J.; Bartlett, D. C.; Weston, C. J.; Curbishley, S. M.; Haughton, E.; Williams, K. T.; Reynolds, G. M.; Newsome, P. N.; Adams, D. H.; Afford, S. C. Isolation of primary human hepatocytes from normal and diseased liver tissue: A one hundred liver experience. PLoS ONE 6(3):e18222; 2011.

5. Bonora-Centelles, A.; Donato, M. T.; Lahoz, A.; Pareja, E.; Mir, J.; Castell, J. V.; Gómez-Lechón, M. J. Functional characterization of hepatocytes for cell transplantation: Customized cell preparation for each receptor. Cell Transplant. 19(1):21–28; 2010.

6. Carpentier, B.; Gautier, A.; Legallais, C. Artificial and bioartificial liver devices: Present and future. Gut 58(12): 1690–1702; 2009.

7. Christoforidis, D.; Martinet, O.; Lejeune, F. J.; Mosimann, F. Isolated liver perfusion for nonresectable liver tumours: A review. Eur. J. Surg. Oncol. 28(8):875–890; 2002.

8. Delriviere, L.; Gibbs, P.; Kobayashi, E.; Goto, S.; Kamada, N.; Gianello, P. Detailed modification technique for safer harvesting and preparation of liver graft in the rat. Microsurgery 17(12):690–696; 1996.

9. Demetriou, A. A.; Brown, R. S.; Busuttil, R. W.; Fair, J.; McGuire, B. M.; Rosenthal, P.; Esch, J. S. A.; Lerut, J.; Nyberg, S. L.; Salizzoni, M.; Fagan, E. A.; de Hemptinne, B.; Broelsch, C. E.; Muraca, M.; Salmeron, J. M.; Rabkin, J. M.; Metselaar, H. J.; Pratt, D.; De La Mata, M.; McChesney, L. P.; Everson, G. T.; Lavin, P. T.; Stevens, A. C.; Pitkin, Z.; Solomon, B. A. Prospective, randomized, multicenter, controlled trial of a bioartificial liver in treating acute liver failure. Ann. Surg. 239(5):660–667; 2004.

10. Dunn, J. C.; Tompkins, R. G.; Yarmush, M. L. Long-term in vitro function of adult hepatocytes in a collagen sandwich configuration. Biotechnol. Progr. 7(3):237–245; 1991.

11. Everson, G. T.; Kulig, C. C. Antiviral therapy for hepatitis C in the setting of liver transplantation. Curr. Treat. Options Gastroenterol. 9(6):520–529; 2006.

12. Ferrigno, A.; Rizzo, V.; Boncompagni, E.; Bianchi, A.; Gringeri, E.; Neri, D.; Richelmi, P.; Freitas, I.; Cillo, U.; Vairetti, M. Machine perfusion at 20°C reduces preservation damage to livers from nonheart beating donors. Cryobiology 62(2):152–158; 2011.

13. Fisher, R. A.; Strom, S. C. Human hepatocyte transplantation: Worldwide results. Transplantation 82(4):441–449; 2006.

14. Fondevila, C.; Hessheimer, A. J.; Flores, E.; Ruiz, A.; Mestres, N.; Calatayud, D.; Paredes, D.; Rodriguez, C.; Fuster, J.; Navasa, M.; Rimola, A.; Taura, P.; Garcia-Valdecasas, J. C. Applicability and results of Maastricht Type 2 donation after cardiac death liver transplantation. Am. J. Transplant. 12(1):162–170; 2011.

15. Fondevila, C.; Hessheimer, A. J.; Maathus, M. H. J.; Munoz, J.; Taura, P.; Calatayud, D.; Leuvenink, H.; Rimola, A.; Ploeg, R. J.; García-Valdecasas, J. C. Superior preservation of DCD livers with continuous normothermic perfusion. Ann. Surg. 254:1000–1007; 2011.

16. Fukumori, T.; Kato, T.; Levi, D.; Olson, L.; Nishida, S.; Ganz, S.; Nakamura, N.; Madariaga, J.; Ohkohchi, N.; Satomi, S.; Miller, J.; Tzakis, A. Use of older controlled nonheart beating donors for liver transplantation. Transplantation 75(8):1171–1174; 2003.

17. Galvao, F. H. F.; de Andrade, D. R.; de Andrade, D. R.; Martins, B. C.; Marson, A. G.; Bernard, C. V.; dos Santos, S. A.; Bacchella, T.; Machado, M. C. C. Hepatocyte transplantation: State of the art. Hepatol. Res. 36(4):237–247; 2006.

18. Garcia-Valdecasas, J. C.; Fondevila, C. In-vivo normothermic recirculation. Curr. Opin. Organ Transplant. 15(2):173–176; 2010.

19. Gómez-Lechón, M. J.; Castell, J. V.; Donato, M. T. Hepatocytes—the choice to investigate drug metabolism and toxicity in man: In vitro variability as a reflection of in vivo. Chem. Biol. Interact. 168(1):30–50; 2007.

20. Gómez-Lechón, M. J.; Donato, M. T.; Castell, J. V.; Jover, R. Human hepatocytes as a tool for studying toxicity and drug metabolism. Curr. Drug Metab. 4(4):292–312; 2003.

21. Gómez-Lechón, M. J.; Donato, T.; Ponsoda, X.; Castell, J. V. Human hepatic cell cultures: In vitro and in vivo drug metabolism. Altern. Lab. Anim. 31(3):257–265; 2003.

22. Gore, A.; Li, Z.; Fung, H. L.; Young, J. E.; Agarwal, S.; Antosiewicz-Bourget, J.; Canto, I.; Giorgetti, A.; Israel, M. A.; Kiskinis, E.; Lee, J. H.; Loh, Y. H.; Manos, P. D.; Montserrat, N.; Panopoulos, A. D.; Ruiz, S.; Wilbert, M. L.; Yu, J.; Kirkness, E. F.; Izpisua Belmonte, J. C.; Rossi, D. J.; Thomson, J. A.; Eggan, K.; Daley, G. Q.; Goldstein, L. S.; Zhang, K. Somatic coding mutations in human induced pluripotent stem cells. Nature 471(7336):63–67; 2011.

23. Guarrera, J. V.; Henry, S. D.; Chen, S. W.; Brown, T.; Nachber, E.; Arrington, B.; Boykin, J.; Samstein, B.; Brown, R. S. J.; Emond, J. C.; Lee, H. T. Hypothermic machine preservation attenuates ischemia/reperfusion markers after liver transplantation: Preliminary results. J. Surg. Res. 167(2):e365–e373; 2011.

24. Han, D. W.; Tapia, N.; Joo, J. Y.; Greber, B.; Arauzo-Bravo, M. J.; Bernemann, C.; Ko, K.; Wu, G.; Stehling, M.; Do, J. T.; Scholer, H. R. Epiblast stem cell subpopulations represent mouse embryos of distinct pregastrulation stages. Cell 143(4):617–627; 2010.

25. Hughes, R. D.; Mitry, R. R.; Dhawan, A. A.; Lehec, S. C.; Girlanda, R.; Rela, M.; Heaton, N. D.; Muiesan, P. Isolation of hepatocytes from livers from nonheart beating donors for cell transplantation. Liver Transpl. 12:713–717; 2006.

26. Hui, S.; Parsons, D. F. Phase transition of plasma membranes of rat hepatocyte and hepatoma cells by electron diffraction. Cancer Res. 36:1918–1922; 1976.

27. Izamis, M. L.; Sharma, N. S.; Uygun, B.; Bieganski, R.; Saeidi, N.; Nahmias, Y.; Uygun, K.; Yarmush, M. L.; Berthiaume, F. In situ metabolic flux analysis to quantify the liver metabolic response to experimental burn injury. Biotechnol. Bioeng. 108(4):839–852; 2010.

28. Kamiike, W.; Burdelski, M.; Steinhoff, G.; Ringe, B.; Lauchart, W.; Pichlmayr, R. Adenine nucleotide metabolism and its relation to organ viability in human liver transplantation. Transplantation 45(1):138–143; 1988.

29. Kamiike, W.; Watanabe, F.; Hashimoto, T.; Tagawa, K.; Ikeda, Y.; Nakao, K.; Kawashima, Y. Changes in cellular levels of ATP and its catabolites in ischemic rat liver. J. Biochem. 91(4):1349–1356; 1982.

30. Kanoria, S.; Jalan, R.; Seifalian, A. M.; Williams, R.; Davidson, B. R. Protocols and mechanisms for remote ischemic preconditioning: A novel method for reducing ischemia reperfusion injury. Transplantation 84(4):445–458; 2007.

31. Kerkweg, U.; Tongju, L.; de Groot, H.; Rauen, U. Cold-induced apoptosis of rat liver cells in University of Wisconsin Solution: The central role of chelatable iron. Hepatology 35:560–567; 2002.

32. Klein, A. S.; Messersmith, E. E.; Ratner, L. E.; Kochik, R.; Baliga, P. K.; Ojo, A. O. Organ donation and utilization in the United States, 1999–2008. Am. J. Transplant. 10(Part 2):973–986; 2010.

33. Lanir, A.; Jenkins, R. L.; Caldwell, C.; Lee, R. G. L.; Khettry, U.; Clouse, M. E. Hepatic transplantation survival: Correlation with adenine nucleotide level in donor liver. Hepatology 8(3):471–475; 1988.

34. Lecluyse, E. L.; Alexandre, E. Isolation and culture of primary hepatocytes from resected human liver tissue. Methods Mol. Biol. 640:57–82; 2010.

35. Lee, C. Y.; Jain, S.; Duncan, H. M.; Zhang, J. X.; Jones, J. W., Jr.; Southard, J. H.; Clemens, M. G. Survival transplantation of preserved nonheart beating donor rat livers: Preservation by hypothermic machine perfusion. Transplantation 76(10):1432–1436; 2003.

36. Lee, C. Y.; Zhang, J.; deSilva, H.; Coger, R.; Clemens, M. Heterogeneous flow patterns during hypothermic machine perfusion preservation of livers. Transplantation 70(12):1797–1802; 2000.

37. Montalvo-Jave, E. E.; Escalante-Tattersfield, T.; Ortega-Salgado, J. A.; Piña, E.; Geller, D. A. Factors in the pathophysiology of the liver ischemia-reperfusion injury. J. Surg. Res. 147(1):153–159; 2008.

38. Nagrath, D.; Xu, H.; Tanimura, Y.; Zuo, R.; Berthiaume, F.; Avila, M.; Yarmush, R.; Yarmush, M. L. Metabolic preconditioning of donor organs: Defatting fatty livers by normothermic perfusion ex vivo. Metab. Eng. 11(4–5): 274–283; 2009.

39. Oertel, M.; Menthena, A.; Chen, Y. Q.; Shafritz, D. A. Properties of cryopreserved fetal liver stem/progenitor cells that exhibit long-term repopulation of the normal rat liver. Stem Cells 24(10):2244–2251; 2006.

40. Olschewski, P.; Gass, P.; Ariyakhagorn, V.; Jasse, K.; Hunold, G.; Menzel, M.; Schöning, W.; Schmitz, V.; Neuhaus, P.; Puhl, G. The influence of storage temperature during machine perfusion on preservation quality of marginal donor livers. Cryobiology 60(3):337–343; 2010.

41. Op den Dries, S.; Sutton, M. E.; Lisman, T.; Porte, R. J. Protection of bile ducts in liver transplantation: Looking beyond ischemia. Transplantation 92(4):373–379; 2011.

42. Organ procurement and transplantation network (accessed 20 July, 2012 URL: optn.transplant.hrsa.gov).

43. Pencavel, T.; Seth, R.; Hayes, A.; Melcher, A.; Pandha, H.; Vile, R.; Harrington, K. J. Locoregional intravascular viral therapy of cancer: Precision guidance for Paris's arrow? Gene Ther. 17(8):946–960; 2010.

44. Perk, S.; Izamis, M. L.; Tolboom, H.; Uygun, B.; Berthiaume, F.; Yarmush, M. L.; Uygun, K. A metabolic index of ischemic injury for perfusion-recovery of cadaveric rat livers. PLoS ONE 6(12):e28518; 2011.

45. Perk, S.; Izamis, M. L.; Tolboom, H.; Uygun, B.; Yarmush, M. L.; Uygun, K. A fitness index for transplantation of machine-perfused cadaveric rat livers. BMC Res. Notes 5(1):325; 2012.

46. Perkins, J. D. Defatting the fatty liver with normothermic perfusion of the liver allograft. Liver Transplant. 15(10):1366–1367; 2009.

47. Pless, G. Bioartificial liver support systems. In: Walker, J. M., ed. Methods in Molecular Biology. Hatfield: Springer Science + Business Media; 2010:511–523.

48. Puppi, J.; Strom, S. C.; Hughes, R. D.; Bansal, S.; Castell, J. V.; Dagher, I.; Ellis, E. C.; Nowak, G.; Ericzon, B. G.; Fox, I. J.; Gómez-Lechón, M. J.; Guha, C.; Gupta, S.; Mitry, R. R.; Ohashi, K.; Ott, M.; Reid, L. M.; Roy-Chowdhury, J.; Sokal, E.; Weber, A.; Dhawan, A. Improving the techniques for human hepatocyte transplantation: Report from a consensus meeting in London. Cell Transplant. 21(1):1–10; 2012.

49. Rauen, U.; Reuters, I.; Fuchs, A.; de Groot, H. Oxygen-free radical-mediated injury to cultured rat hepatocytes during cold incubation in preservation solutions. Hepatology 26:351–357; 1997.

50. Schon, M. R.; Kollmar, O.; Wolf, S.; Schrem, H.; Matthes, M.; Akkoc, N.; Schnoy, N. C.; Neuhaus, P. Liver transplantation after organ preservation with normothermic extracorporeal perfusion. Ann. Surg. 233(1):114–123; 2001.

51. Seglen, P. O. Preparation of isolated rat liver cells. Method Cell Biol. 13:29–83; 1976.

52. Serracino-Inglott, F. H., N. A.; Mathie, R. T. Hepatic ischemia-reperfusion injury. Am. J. Surg. 181(2):160–166; 2001.

53. Soto-Gutierrez, A.; Yagi, H.; Uygun, B. E.; Navarro-Alvarez, N.; Uygun, K.; Kobayashi, N.; Yang, Y. G.; Yarmush, M. L. Cell delivery: From cell transplantation to organ engineering. Cell Transplant. 19(6):655–665; 2010.

54. Tolboom, H.; Izamis, M. L.; Sharma, N.; Milwid, J. M.; Uygun, B.; Berthiaume, F.; Uygun, K.; Yarmush, M. L. Subnormothermic machine perfusion for recovery and preservation of ischemic rat liver grafts. J. Surg. Res. 175(1):149–156; 2012.

55. Tolboom, H.; Milwid, J.; Izamis, M. L.; Uygun, K.; Berthiaume, F.; Yarmush, M. L. Sequential cold storage and normothermic perfusion of the ischemic rat liver. Transplant. Proc. 40(5):1306–1309; 2008.

56. Tolboom, H.; Pouw, R.; Uygun, K.; Tanimura, Y.; Izamis, M. L.; Berthiaume, F.; Yarmush, M. L. A model for normothermic preservation of the rat liver. Tissue Eng. 13(8):2143–2151; 2007.

57. Tolboom, H.; Pouw, R. E.; Izamis, M. L.; Milwid, J. M.; Sharma, N.; Soto-Gutierrez, A.; Nahmias, Y.; Uygun, K.; Berthiaume, F.; Yarmush, M. L. Recovery of warm ischemic rat liver grafts by normothermic extracorporeal perfusion. Transplantation 87(2):170–177; 2009.

58. Totsuka, E.; Fung, U.; Hakamada, K.; Tanaka, M.; Takahashi, K.; Nakai, M.; Morohashi, S.; Nishimura, A.; Ishizawa, Y.; Ono, H.; Toyoki, Y.; Narumi, S.; Sasaki, M. Analysis of clinical variables of donors and recipients with

respect to short-term graft outcome in human liver transplantation. Transplant. Proc. 36(8):2215–2218; 2004.

59. Trevisani, F.; Colantoni, A.; Caraceni, P.; Van Thiel, D. H. The use of donor fatty liver for liver transplantation: A challenge or a quagmire? J. Hepatol. 24(1):114–121; 1996.

60. Uygun, B. E.; Soto-Gutierrez, A.; Yagi, H.; Izamis, M. L.; Guzzardi, M. A.; Shulman, C.; Milwid, J.; Kobayashi, N.; Tilles, A.; Berthiaume, F.; Hertl, M.; Nahmias, Y.; Yarmush, M. L.; Uygun, K. Organ reengineering through development of a transplantable recellularized liver graft using decellularized liver matrix. Nat. Med. 16(7):814–820; 2010.

61. Uygun, K.; Tolboom, H.; Izamis, M. L.; Uygun, B.; Sharma, N. S.; Yagi, H.; Soto-Gutierrez, A.; Hertl, M.; Berthiaume, F.; Yarmush, M. L. Diluted blood reperfusion as a model for transplantation of ischemic rat livers: Alanine aminotransferase is a direct indicator of viability. Transplant. Proc. 42(7):2463–2467; 2010.

62. Vairetti, M.; Ferrigno, A.; Carlucci, F.; Tabucchi, A.; Rizzo, V.; Boncompagni, E.; Neri, D.; Grigneri, E.; Freitas, I.; Cillo, U. Subnormothermic machine perfusion protects steatotic livers against preservation injury: A potential for donor pool increase? Liver Transplant. 15(1):20–29; 2009.

63. Vairetti, M.; Ferrigno, A.; Rizzo, V.; Boncompagni, E.; Carraro, A.; Grigneri, E.; Milanesi, G.; Barni, S.; Freitas, I.; Cillo, U. Correlation between liver temperature employed during machine perfusion and reperfusion damage: Role of Ca^{2+}. Liver Transplant. 14(4):494–503; 2008.

64. van Elten, B.; Eggermont, A. M.; van Tiel, S. T.; Ambagtsheer, G.; de Wilt, J. H.; ten Hagen, T. L. Gene therapy in in vivo isolated perfusion models. Curr. Gene Ther. 5(2):195–202; 2005.

65. Vardanian, A. J.; Busuttil, R. W.; Kupiec-Weglinski, J. W. Molecular mediators of liver ischemia and reperfusion injury. Mol. Med. 14(5–6):337–345; 2007.

66. Vogel, T.; Brockmann, J. G.; Coussios, C.; Friend, P. J. The role of normothermic extracorporeal perfusion in minimizing ischemia reperfusion injury. Transplant. Rev. 26(2):156–162; 2012.

67. Vollmar, B.; Menger, M. D. The hepatic microcirculation: Mechanistic contributions and therapeutic targets in liver injury and repair. Physiol. Rev. 89(4):1269–1339; 2009.

68. White, S. A.; Prasad, K. R. Liver transplantation from non-heart beating donors. Brit. Med. J. 332(7538):376–377; 2006.

69. Yang, Y. G.; Sykes, M. Xenotransplantation: Current status and a perspective on the future. Nat. Rev. Immunol. 7(7):519–531; 2007.